

# Enhancement in the piezoelectric properties of BaTiO<sub>3</sub>–Bi(Mg<sub>1/2</sub>Ti<sub>1/2</sub>)O<sub>3</sub>–BiFeO<sub>3</sub> system ceramics by nanodomain

Ryuta Mitsui<sup>a</sup>, Ichiro Fujii<sup>a</sup>, Kouichi Nakashima<sup>a</sup>, Nobuhiro Kumada<sup>a</sup>,  
Yoshihiro Kuroiwa<sup>b</sup>, Satoshi Wada<sup>a,\*</sup>

<sup>a</sup>Material Science and Technology, Interdisciplinary Graduate School of Medical and Engineering, University of Yamanashi, 4-4-37 Takeda, Kofu, Yamanashi 400-8510, Japan

<sup>b</sup>Department of Physical Science, Hiroshima University, 1-3-1 Kagamiyama, Higashi-Hiroshima, Hiroshima 739-8526, Japan

Available online 22 October 2012

## Abstract

Barium titanate (BaTiO<sub>3</sub>, BT)–bismuth titanate magnesium oxide (Bi(Mg<sub>1/2</sub>Ti<sub>1/2</sub>)O<sub>3</sub>, BMT)–bismuth ferrite (BiFeO<sub>3</sub>, BF) solid solution ceramics were prepared using a conventional solid-state synthesis, and their piezoelectric properties and microstructure were investigated. X-ray diffraction (XRD) patterns revealed the single phase of perovskite oxide for 0.3BT–0.1BMT–0.6BF ceramics. Strain–electric field curves of the sample with 0.3BT–0.1BMT–0.6BF exhibit ferroelectric butterfly-like curves. A strain maximum/electric field maximum ( $S_{\max}/E_{\max}$ ) was 330 pm/V. Transmission electron microscopy revealed dot-like domains (Nanodomains) inside the ferroelectric domain structures in the 0.3BT–0.1BMT–0.6BF.

© 2012 Elsevier Ltd and Techna Group S.r.l. All rights reserved.

**Keywords:** B. Electron microscopy; C. Piezoelectric properties; Perovskites

## 1. Introduction

Lead-free piezoelectrics have extensively been studied due to environmental concerns. Until now, the piezoelectric response and Curie temperature are, however, not simultaneously comparable to those of Pb(Zr,Ti)O<sub>3</sub> [1]. Recently, BaTiO<sub>3</sub>–Bi-based perovskite ceramics have been studied as candidates for lead-free ceramics. The research shows that the Curie temperatures are high, but the piezoelectric responses are small, especially at relaxor compositions [2,3,4]. Therefore, it is necessary to increase the piezoelectric response for practical use. One of the ways to increase the piezoelectric response is the use of contributions from domain wall motion. The domain walls have been known to contribute to dielectric and piezoelectric properties through its vibration and translation [5,6]. Therefore, the piezoelectric response may increase as domain wall density increases, that is, domain size decreases, if the domain wall motion maintains the same. One way to decrease the domain size is to make a solid solution of relaxor and ferroelectric materials. Relaxor is a material distinguished

from ferroelectric in terms of many aspects, as summarized elsewhere. One important distinction is the domain structure called “polar nano region (PNR)”. PNR is mottled and the domains are in nanometer order. Thus, domain size is expected to be decreased from macroscopic ferroelectric domain to microscopic relaxor PNR with increasing relaxor content. In this study, in order to verify the above hypothesis, lead-free relaxor – ferroelectric ceramics with controlled domain size was produced, and the effect of the piezoelectric properties on domain size was investigated. As a model case, barium titanate–bismuth magnesium titanate (BaTiO<sub>3</sub>–Bi(Mg<sub>1/2</sub>Ti<sub>1/2</sub>)O<sub>3</sub>, BT–BMT) and bismuth ferrite (BiFeO<sub>3</sub>, BF) were selected. (1–*x*)BT–*x* BMT (*x*=0.1~0.7) ceramics are relaxor with the dielectric maximum temperature up to 360 °C at *x*=0.5 [4,7]. On the other hand, BF ceramic is a ferroelectric material with a high Curie temperature of ~830 °C. [8]

## 2. Experimental procedure

0.4BT–0.6BMT, 0.45BT–0.2BMT–0.35BF, and 0.3BT–0.1BMT–0.6BF ceramics were prepared by a conventional

\*Corresponding author. Tel.: +60 175272166; fax: +60 46579150.

E-mail address: [swada@yamanashi.ac.jp](mailto:swada@yamanashi.ac.jp) (S. Wada).

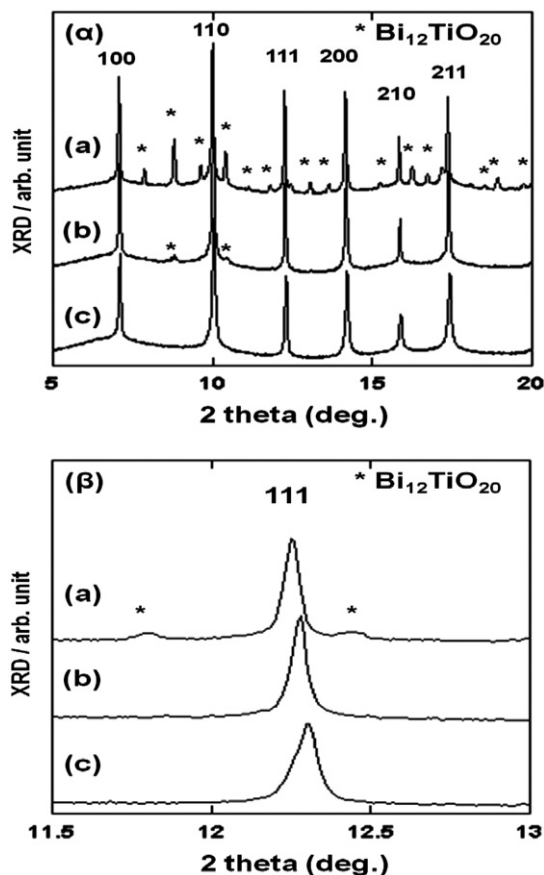


Fig. 1. (A) XRD patterns of sintered samples. (B) (111) peaks (a) 0.4BT–0.6BMT, (b) 0.45BT–0.2BMT–0.35BF, (c) 0.3BT–0.1BMT–0.6BF (Left)  $2\theta=(5\text{--}20^\circ)$  (Right)  $2\theta=(11.5\text{--}13^\circ)$ .

solid state synthesis. The ceramics were hereafter referred to as samples A, B, and C, respectively. Powders of barium titanate ( $\text{BaTiO}_3$ , BT01, Sakai Chemical Industry Co., Ltd.), bismuth oxide ( $\text{Bi}_2\text{O}_3$ , 99.999%, Rare Metallic Co., Ltd.), magnesium oxide ( $\text{MgO}$ , 99.9%, Rare Metallic Co., Ltd.), titanium oxide ( $\text{TiO}_2$ , MPT-851, Ishihara Sangyo Kaisha, Ltd.), and  $\alpha$ -iron oxide ( $\alpha\text{-Fe}_2\text{O}_3$ , 99.99%, Rare Metallic Co., Ltd.) were weighed and ball-milled with zirconia balls and ethanol for 16 h. After drying at  $80^\circ\text{C}$ , the powders were ground and calcined at  $900^\circ\text{C}$  for 6 h in air. The crystal structure of calcined powders was checked by X-ray diffraction (XRD) (RINT2000, Rigaku Corporation) with  $\text{Cu K}\alpha$  radiation. The powders were again ground and ball-milled for 16 h. After drying at  $80^\circ\text{C}$ , the powder was mixed with 3 wt% polyvinyl butyral. Obtained powders were ground and sieved through a  $250\text{ }\mu\text{m}$  mesh screen. The powders were uniaxially pressed at 320 MPa in a 10-mm-diameter die. After binder burnout at  $700^\circ\text{C}$ , the compacts were sintered at  $950\text{--}1000^\circ\text{C}$  for 2 h in air. The densities of the samples were measured by an Archimedes method. The densities of the samples were found to be more than 94% of the theoretical ones. For crystal structure characterization, the sintered samples were crushed into powders and they were annealed at  $700^\circ\text{C}$ . The crystal structure and lattice parameter of the powders were determined using a synchrotron X-ray source (BL02B2, SPring-8) with the wavelength of  $0.49417\text{ }\text{\AA}$ . Microstructure of the samples was observed by transmission electron microscopy (TEM) (Tecnai F30, FEI Company) operated at 300 kV. A traditional

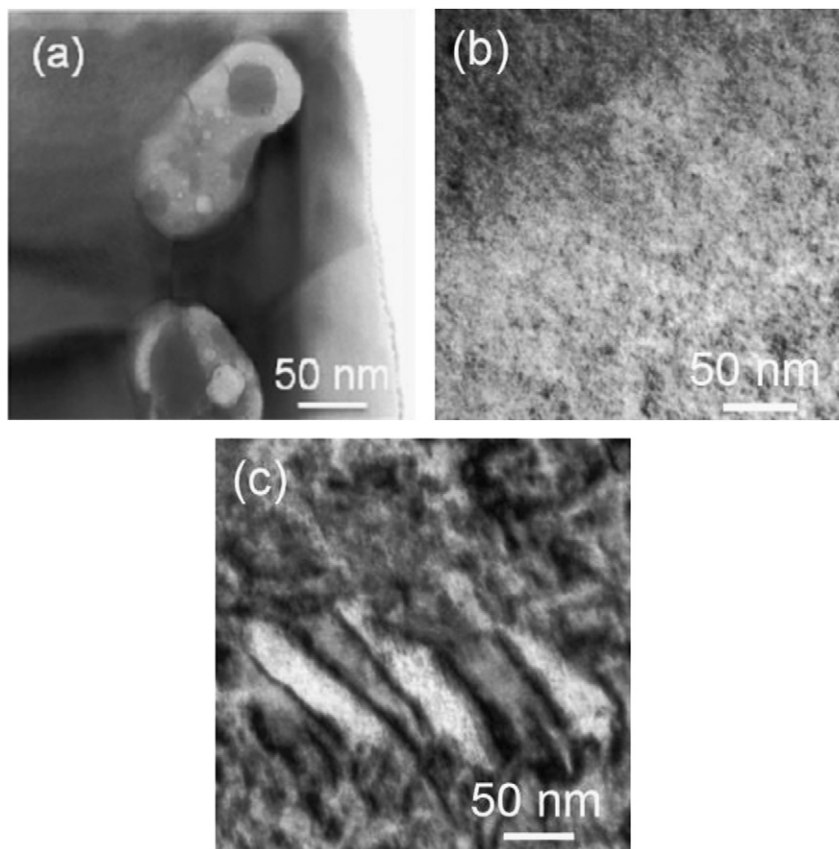


Fig. 2. Bright-field TEM photograph of domain structure in the samples: (a) 0.4BT–0.6BMT (b) 0.45BT–0.2BMT–0.35BF, and (c) 0.3BT–0.1BMT–0.6BF.

procedure including polishing and ion-milling was used for TEM sample preparation. For electric characterizations, the samples were polished down to 0.4 mm in thickness. Gold electrodes were sputtered on the top and bottom surfaces. The samples were sawed into the size of 4 mm × 1.5 mm × 0.4 mm. The dielectric constant and loss were measured using an LCR meter (6440B, Wayne Kerr Electronics), with increasing temperature from room temperature to 500 °C with a heating rate of 3 °C/min. Polarization–electric field (P–E) and strain–electric field (S–E) curves were measured at room temperature using ferroelectric characteristics evaluation systems. Apparent, or large-field, piezoelectric constant,  $d_{33}^*$ , was defined as maximum strain over the applied electric field amplitude of 50 kV/cm observed in the S–E curve.

### 3. Results and discussion

Fig. 1 (A) shows synchrotron XRD patterns of the samples. The crystal structure of samples A and B was mixed phases of a pseudo-cubic perovskite oxide and  $\text{Bi}_{12}\text{TiO}_{20}$ , while that of sample C was the single-phase pseudo-cubic perovskite. The amount of the  $\text{Bi}_{12}\text{TiO}_{20}$  phase reduced and eventually disappeared as the BMT content decreased. This is because BMT was only stable when it was prepared at high pressure [9], otherwise, it will decompose into phases including  $\text{Bi}_{12}\text{TiO}_{20}$ , although the solid solution with  $\text{BaTiO}_3$  stabilizes the perovskite phase [4]. Fig. 1 (b) shows the pseudo-cubic (1 1 1) peak of the samples, it was found that the peaks of samples A and B were symmetric, while that of sample C was asymmetric with a small shoulder on the left-hand side. Since the crystal structure of BF is rhombohedral at room temperature, this indicates that the crystal structure of sample C includes the influence of rhombohedral distortion. The lattice parameter of the pseudo-cubic perovskite phase of samples A, B, and C was calculated to be 4.0124 Å, 4.0064 Å, and 3.9983 Å, respectively. It was likely that the decrease in the lattice parameter with the BF content was associated with smaller lattice parameters of BF.

Microstructure was observed by TEM. Fig. 2 shows bright-field TEM images of the samples. The microstructure depended on the composition, and domain size reduced as the BF content decreased. Macroscopic, ferroelectric-like domain patterns were observed for sample C (Fig. 2(c)). On the other hand, such a domain pattern was not observed for samples A and B (Fig. 2(a)). The absence of such a macroscopic domain structure was associated with a relaxor characteristic. Regarding the sample B, a mottled pattern was observed (Fig. 2(b)).

It is likely that the white regions were nano-sized domains and the dark regions were domain walls. The domain patterns observed for the samples are consistent with the XRD results, the pseudo-cubic, symmetric (1 1 1) peak for relaxor-like samples A and B, while asymmetric one for ferroelectric sample C includes the influence of rhombohedral distortion.

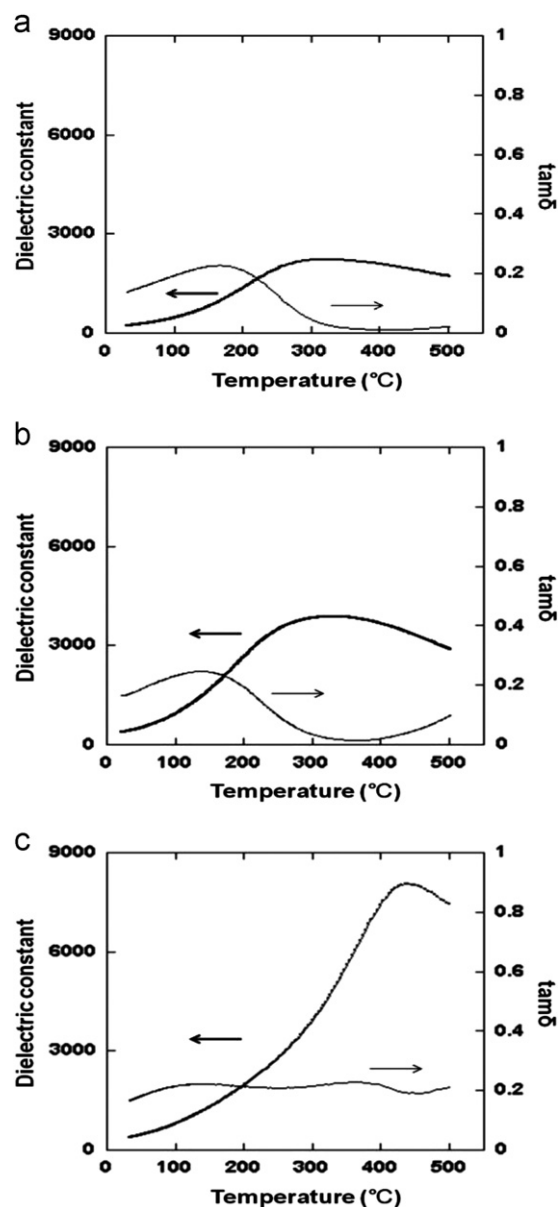


Fig. 3. The temperature dependence of the dielectric properties of the samples (a) 0.4BT–0.6BMT  $T_{\text{Max}} = 320$  °C at 1 MHz (b) 0.45BT–0.2BMT–0.35BF  $T_{\text{Max}} = 330$  °C at 1 MHz, and (c) 0.3BT–0.1BMT–0.6BF  $T_{\text{Max}} = 440$  °C at 3 MHz.

Temperature dependence of the dielectric properties of samples A and B at 1 MHz, C at 3 MHz is shown in Fig. 3. A broad peak was observed for the dielectric constant profiles. The peak of samples A and B was broad, and such a peak was reported for relaxor BT–Bi-based perovskite oxide [2,3,4]. On the other hand, the peak of sample C was sharper than the samples A and B. As a result it seems that the sample C mixes with ferroelectrics and relaxor phase. As the BF content increased, the peak temperature increased, that is, 320 °C, 330 °C, and 440 °C for samples A, B, and C, respectively. This is attributed to the high Curie temperature of the BF.

Figs. 4 and 5, show the room temperature P–E hysteresis loops and S–E curves for samples A, B and C measured at

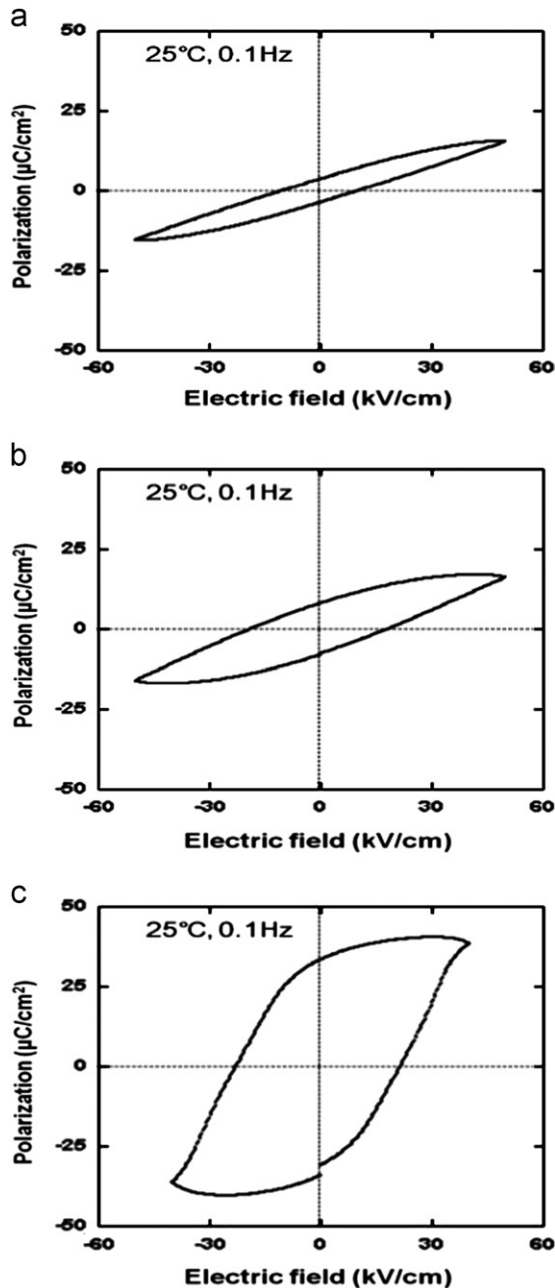


Fig. 4. P–E hysteresis loops of the samples (a) 0.4BT–0.6BMT, (b) 0.45BT–0.2BMT–0.35BF, and (c) 0.3BT–0.1BMT–0.6BF.

0.1 Hz, respectively. P–E hysteresis loops of sample A and B were slim with a relaxor-like form. On the other hand, the P–E hysteresis loop of sample C possesses larger remanent polarization and coercive field, compared with the samples A and B. For the S–E curves, a ferroelectric butterfly curve was observed for sample C, while a relaxor-like with quadratic curve was observed for samples A and B. The apparent piezoelectric constant,  $d_{33}^*$ , was 44, 128, and 330 pm/V for samples A, B, and C, respectively. Therefore, the value of  $d_{33}^*$  of the sample B with nano-sized domains (Fig. 2(c)) was lower than that of the sample

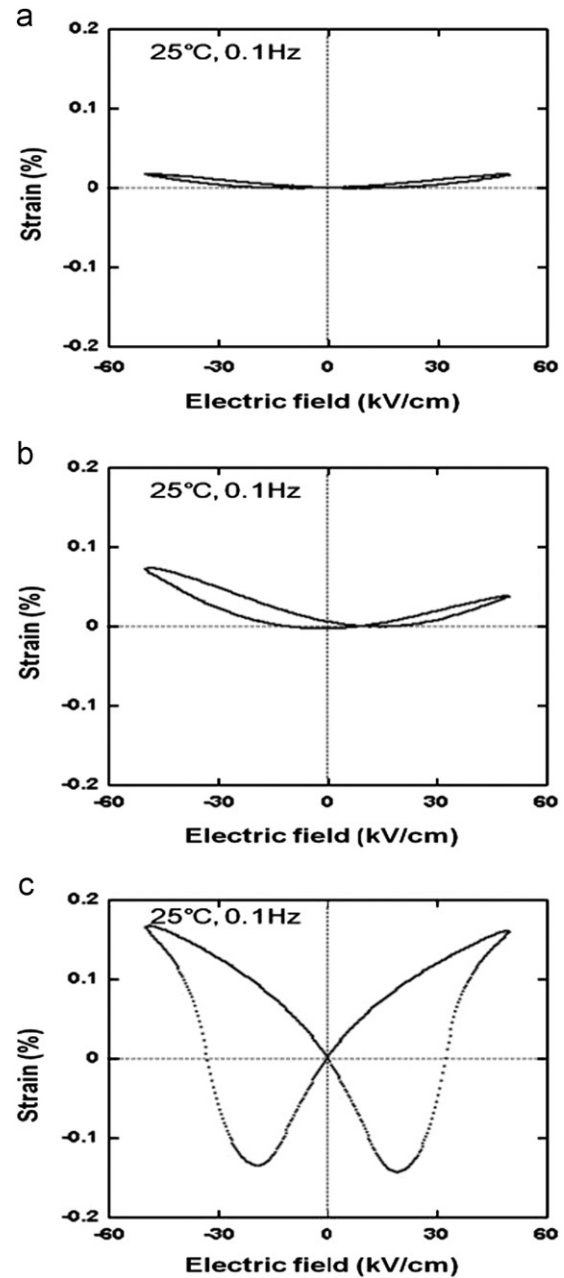


Fig. 5. Bipolar S–E curves of the samples (a) 0.4BT–0.6BMT, (b) 0.45BT–0.2BMT–0.35BF, and (c) 0.3BT–0.1BMT–0.6BF.

C. Thus, this result indicates that the Nanodomain did not increase the piezoelectric response. In this study, only three compositions were studied for a wide composition range of the ternary system. Since the domain wall density is believed to increase at compositions where the characteristics change from ferroelectric to relaxor, research in a narrow composition range near sample C is necessary to confirm the effect of Nanodomain.

#### 4. Conclusions

The dielectric and piezoelectric properties of 0.4 BT–0.6BMT, 0.45BT–0.2BMT–0.35BF, and 0.3BT–0.1

BMT–0.6BF ceramics were investigated. As the BF content increases, the dielectric constant peak temperature increases and the properties change from relaxor to ferroelectric. In microstructure observation, for 0.4BT–0.6BMT composition no macroscopic domain pattern was found. Nano-sized domain structure was observed for 0.45BT–0.2BMT–0.35BF composition. However, high piezoelectric properties were not observed. Ferroelectric-like domain patterns were observed 0.3BT–0.1BMT–0.6BF composition. The piezoelectric properties were the largest in the three compositions.

## References

- [1] T.R. Shrout, S.J. Zhang, Lead-free piezoelectric ceramics: alternatives for PZT?, *Journal of Electroceramics* 19 (2007) 111–124.
- [2] C.C. Huang, D.P. Cann, Phase transitions and dielectric properties in  $\text{Bi}(\text{Zn}_{1/2}\text{Ti}_{1/2})\text{O}_3$ – $\text{BaTiO}_3$  perovskite solid solutions, *Journal of Applied Physics* 104 (2008) 024117.
- [3] S.O. Leontsev, R.E. Eitel, Dielectric and piezoelectric properties in Mn-modified  $(1-x)\text{BiFeO}_3-x\text{BaTiO}_3$  ceramics, *Journal of the American Ceramic Society* 92 (2009) 2957–2961.
- [4] S. Wada, Piezoelectric properties of high Curie temperature barium titanate–bismuth perovskite-type oxide system ceramics, *Journal of Applied Physics* 108 (2010) 094114.
- [5] G. Arlt, The role of domain walls on the dielectric, elastic and piezoelectric properties of ferroelectric ceramics, *Ferroelectrics* 76 (1987) 451–458.
- [6] S.P. Li., W.W. Cao, L.E. Cross, The extrinsic nature of nonlinear behavior observed in lead zirconate titanate ferroelectric ceramic, *Journal of Applied Physics* 69 (1991) 7219–7224.
- [7] I. Fujii, Relaxor characteristics of  $\text{BaTiO}_3$ – $\text{Bi}(\text{Mg}_{1/2}\text{Ti}_{1/2})\text{O}_3$  ceramics, *Key Engineering Materials* 485 (2011) 31–34.
- [8] M.M. Kumar, V.R. Palkar, K. Srinivas, S.V. Suryanarayana, Structure property relations in  $\text{BiFeO}_3/\text{BaTiO}_3$  solid solutions, *Applied Physics Letters* 76 (2000) 2764–2766.
- [9] Y. Inaguma, A. Miyaguchi, T. Katsumata, Synthesis and lattice distortion of ferroelectric/antiferroelectric Bi(III)-containing perovskites, *Materials Research Society Symposium Proceedings* 755 (2003) 471–476.